Robust and Nonrobust Impacts of Atmospheric Cloud-Radiative Interactions on the Tropical Circulation and Its Response to Surface Warming

Nicole Albern[1,2] (ID), Aiko Voigt[2,3] (ID), Stefan A. Buehler[1] (ID), and Verena Grützun[1]

[1]Meteorologisches Institut, Universität Hamburg, Hamburg, Germany, [2]Institute of Meteorology and Climate Research — Department Troposphere Research, Karlsruhe Institute of Technology, Karlsruhe, Germany, [3]Lamont-Doherty Earth Observatory, Columbia University, New York, NY, USA

Abstract The impact of cloud-radiative interactions on the tropical circulation and its response to surface warming are studied in aquaplanet model simulations with prescribed sea-surface temperatures from eight global atmosphere models. Simulations with enabled and disabled cloud-radiative interactions are compared. In a present-day-like climate, the presence of cloud-radiative interactions strengthens the Hadley cell, narrows and strengthens tropical ascent, and widens subtropical descent. These cloud impacts are robust across models and are shown to be related to the energetics and mass constraints of the tropical atmosphere. Cloud-radiative interactions have no robust impact on the circulation response to surface warming but amplify model differences in the response of the ascent and the Hadley cell strength. The lack of robust cloud impacts is consistent with the fact that surface warming-induced changes in atmospheric cloud-radiative effects are small compared to the cloud-radiative effects in the present-day-like climate.

Plain Language Summary The atmospheric circulation is crucial for the global and regional climate and climate change. A main source of uncertainty in climate models is clouds. An important way of how clouds impact the circulation is by absorbing, emitting, and scattering radiation. We study the impact of cloud-radiative interactions on the tropical circulation by considering an ensemble of climate models that simulate a water-covered aquaplanet. In one set of simulations, clouds fully interact with radiation. In another set, clouds are made transparent to radiation, which disables cloud-radiative interactions. We find that cloud-radiative interactions strengthen the tropical Hadley circulation, narrow and strengthen the regions of upward motion, and widen the regions of downward motion. We relate these cloud impacts to basic energetics and mass constraints of the tropical atmosphere. In response to increasing surface temperatures, cloud-radiative interactions have no robust impact on the circulation across the models but amplify model differences. Our results help to better understanding the role of clouds in the climate system and contribute to the World Climate Research Programme's Grand Challenge on Clouds, Circulation, and Climate Sensitivity.

1. Introduction

Recent work showed that cloud-radiative interactions play an important role for the tropical circulation of the atmosphere. In particular, atmospheric cloud-radiative effects (ACRE; the difference between top-of-atmosphere and surface values of all-sky minus clear-sky radiative fluxes) were shown to narrow the Intertropical Convergence Zone (ITCZ). Various mechanisms have been put forward to explain the cloud-induced narrowing based on moist static energy considerations (Fläschner, 2016; Harrop & Hartmann, 2016; Popp & Silvers, 2017). Harrop and Hartmann (2016) used the upper-level moist static energy to propose that the tropical upper-tropospheric heating by cloud-radiative interactions decreases convective available potential energy and postpones the onset of convection to latitudes closer to the equator. Popp and Silvers (2017) analyzed lower-level and vertically integrated moist static energy to suggest that the cloud-induced strengthening of the Hadley circulation leads to higher boundary layer moist static energies near the equator, and hence a narrower ITCZ. Fläschner (2016) started from the vertical-mean moist static energy to argue that the ITCZ narrowing is caused by a small equatorward displacement of ACRE with respect to the moist static energy maximum.

In this study, we propose an alternative view on how cloud-radiative interactions affect the ITCZ and, more generally, the tropical circulation. To this end, we idealize the tropical atmosphere as a two-box model, with one box representing the ascent region and one box representing the descent region (Byrne & Schneider, 2016a, 2016b). This allows us to qualitatively explain those cloud-radiative impacts that are robust across global models from basic energetics and mass constraints of the tropical atmosphere. Our interest here is in providing reasons for the robust qualitative impacts of ACRE. The arguments we put forward involve several approximations and, as a result, are found to be less suited to rationalize quantitative model differences in the ACRE impact.

Investigations of the cloud-radiative impact date back to at least Slingo and Slingo (1988), Randall et al. (1989), and Sherwood et al. (1994). Here we follow recent work that has made use of idealized aquaplanet simulations in which cloud-radiative interactions are included, and simulations in which clouds are made transparent to radiation. The latter disables cloud-radiative interactions. These simulations are part of the Clouds On-Off Klimate Intercomparison Experiment (COOKIE; Stevens et al., 2012). Aquaplanet simulations with comprehensive physics models highlight the impact of moist atmospheric processes related to convection and clouds. This makes them a useful test bed to study the fundamental mechanisms by which cloud-radiative interactions impact the tropical circulation. Extending previous studies, we provide a thorough characterization of the cloud-radiative impact on tropical precipitation and the Hadley circulation. This is important as the Hadley circulation shapes tropical and subtropical precipitation and Earth's radiation balance (Su et al., 2014). We also study the subsiding part of the tropical circulation, which affects the net precipitation pattern in the subtropics (Scheff & Frierson, 2012).

Clouds and their radiative interactions change as the climate warms. In climate models, cloud-radiative interactions and their response to climate change are important in setting the circulation response to climate change (Ceppi & Hartmann, 2016; Ceppi & Shepherd, 2017; Voigt et al., 2014; Voigt & Shaw, 2015, 2016). Besides aquaplanet simulations with present-day-like sea-surface temperatures (SSTs), COOKIE includes simulations with increased SSTs. This allows us to investigate to what extent the impact of cloud-radiative interactions depends on the climate state and to what extent changes in cloud-radiative interactions affect the circulation response to surface warming. Previous work using COOKIE focused on simulations with present-day-like SSTs.

2. Simulations and Circulation Metrics

2.1. COOKIE Simulations and Additional Simulations With the ICON Model

The COOKIE aquaplanet simulations (Stevens et al., 2012) follow the Coupled Model Intercomparison Project Phase 5 aquaplanet protocol (Neale & Hoskins, 2001; Taylor et al., 2012). In the control (CTRL) simulation, SSTs are set to the zonally-uniform *Qobs* profile. In the *4K* simulations, SSTs are increased everywhere by 4K to mimic global warming. Two versions of CTRL and 4K are available to study the role of cloud-radiative interactions. In onCTRL and on4K, clouds interact with radiation (clouds-on). In offCTRL and off4K, clouds are made transparent to radiation (clouds-off). Because SSTs are prescribed, the aquaplanet setup isolates the impact of ACRE. The six atmospheric general circulation models that have provided the COOKIE simulations with CTRL and 4K SSTs are used here (Table 1). All months available from the Earth System Grid Federation (https://esgf-data.dkrz.de/) and Climate and Environmental Retrieval and Archive (https://cera-www.dkrz.de/) archives are used, with the first 6 months discarded to remove model initialization effects.

We further performed COOKIE aquaplanet simulations with two versions of the ICOsahedral Nonhydrostatic model (ICON; Zängl et al., 2015). ICON did not contribute to the original COOKIE data set. The two versions of ICON use the same dynamical core but differ in the parameterizations of subgrid-scale physical processes, such as clouds, convection, and radiation. This provides us with an opportunity to assess the impact of physical parameterizations. The two ICON versions apply the physics packages used for numerical weather prediction (ICON-DWD; developed by the German Weather Service; version 2.0.15) and climate simulation (ICON-MPI; developed by the Max Planck Institute for Meteorology; version 2.1.00). The simulations are performed in R2B04 resolution (160 km horizontal resolution). For ICON-DWD, 60 levels extending up to 75 km and a time step of 1,440 s are used. For ICON-MPI, 47 levels extending up to 83 km and a time step of 600 s are used. We ran both versions for a simulated time of 10 years, with the first 6 months excluded from the analysis.

Table 1
Impact of the Presence of Cloud-Radiative Interactions on the Tropical Circulation in the Present-Day-Like Climate

	Model	Ψ	$\bar{\omega}^{\uparrow}$	$\bar{\omega}^{\downarrow}$	φ^{HC}	$\varphi^{\uparrow}$	$\varphi^{\downarrow}$	$\bar{P}$	P_{max}
A	CNRM-CM5	53.4/40.2	11.1/9.4	5.7/2.9	−3.0/−1.7	−4.6/−4.0	1.6/2.3	−0.1/−0.1	1.0/0.3
B	HadGEM2-A	46.5/19.0	17.5/9.7	−0.2/−0.5	0.3/0.4	−2.3/−1.4	2.7/1.8	−0.1/−0.2	3.1/2.2
C	IPSL-CM5A-LR	−21.8/−4.0	2.7/2.4	−3.5/−2.4	−1.4/−0.5	−1.8/−1.6	0.4/1.2	−0.5/−0.6	0.2/0.0
D	MIROC5	93.7/59.9	30.8/25.4	1.5/−0.5	−2.4/−2.8	−7.5/−7.8	5.1/5.0	−0.2/−0.4	7.5/6.0
E	MPI-CM5-LR	63.9/75.4	15.6/25.5	2.2/1.3	−1.3/−1.7	−5.0/−7.7	3.7/6.0	−0.1/−0.3	2.7/9.2
F	MRI-CGCM3	15.5/9.2	13.8/12.4	−2.2/−2.0	0.4/0.3	−1.9/−1.5	2.3/1.8	−0.3/−0.3	7.8/9.1
Ga	ICON-DWD	10.5/30.4	4.7/10.5	−0.6/−1.6	0.0/0.2	−1.5/−3.1	1.5/3.3	−0.1/−0.2	0.6/2.4
Gb	ICON-MPI	24.8/19.4	4.7/4.9	0.5/−0.2	−0.1/0.2	−1.6/−2.1	1.5/2.2	−0.2/−0.3	0.8/1.7

Note. The numbers are calculated from the clouds-on minus the clouds-off simulations. The first number is for the control simulations and the second for the 4K simulations. Ψ is the Hadley circulation strength in 10^9 kg/s, $\bar{\omega}^{\uparrow}$, and $\bar{\omega}^{\downarrow}$ are the magnitude of ascent and descent in hectopascal per day, φ^{HC} is the width of the Hadley cell in degree latitude, and $\varphi^{\uparrow}$ and $\varphi^{\downarrow}$ are the width of the ascent and descent in degree latitude. $\bar{P}$ and P_{max} are the tropical-mean (within 30° N/S) and the peak precipitation in millimeter per day.

2.2. Hadley Circulation Metrics

We idealize the tropical circulation as a two-box model, with ascending motion, deep convection, and high-level clouds in the equatorial box and descending motion, shallow convection, and low-level clouds in the subtropical box (e.g., Byrne & Schneider, 2016b; Pierrehumbert, 1995). Figure 1 illustrates the two-box model and the aspects of the Hadley circulation that we investigate in this paper. Because the Northern and Southern Hemispheres are statistically identical, we average over the two hemispheres. Whereas previous COOKIE studies focused on the ITCZ and precipitation, we study the tropical circulation in terms of the Hadley cell and its ascending and descending branches. The Hadley cell width and strength are characterized by the zonal-mean time-mean meridional mass stream function. The Hadley cell width φ^{HC} is defined as the distance between the equator and the first poleward zero crossing of the mass stream function at 500 hPa, using linear interpolation to account for the models' latitudinal grids. The Hadley cell strength Ψ is measured as the maximum absolute value of the mass stream function between the equator and 30° N/S and between 850 and 200 hPa.

The width and strength of the ascending and descending branches of the Hadley cell are characterized through the vertical pressure velocity ω. Following Medeiros et al. (2015), the ascent and descent strengths, $\bar{\omega}^{\uparrow}$ and $\bar{\omega}^{\downarrow}$, are defined as the absolute values of the time-mean area-mean negative and positive ω within 30° N/S and averaged between 850 and 200 hPa. Because we take the absolute values, an increase in $\bar{\omega}^{\uparrow}$ and $\bar{\omega}^{\downarrow}$ implies stronger ascent or descent, respectively. The ascent width $\varphi^{\uparrow}$ is defined as the distance between the equator and the first poleward zero crossing of ω at 500 hPa. Some simulations with a double ITCZ show weak descending motions around the equator. In these cases, the ascent width is nonetheless measured with respect to the equator. The descent width $\varphi^{\downarrow}$ is given by the distance between the poleward edge of the ascent and the edge of the Hadley cell. We also considered an alternative metric for descent width, namely, the distance between the poleward edge of the ascent and the next poleward zero crossing of ω at 500 hPa, which includes part of the Ferrel cell and comprises the subtropical dry zone. We found that the two metrics are highly correlated (correlation coefficients > 0.84), and so we only report the first metric that focuses on the Hadley cell.

The circulation metrics are summarized in Figure 1 and Table 1. Some of our arguments presented below include the tropical-mean (average within 30° N/S) and peak precipitation, $\bar{P}$ and P_{max}. These are included in the tables.
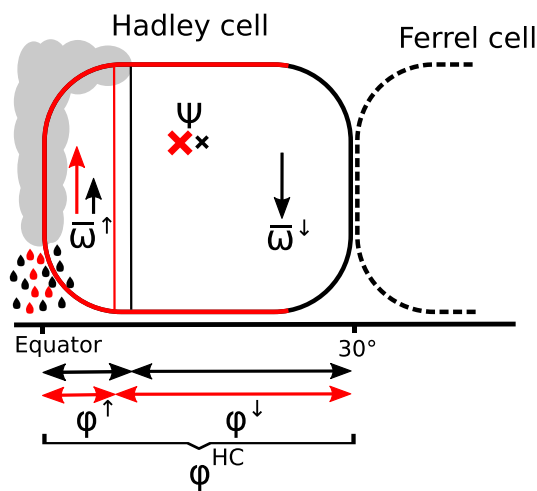

Figure 1. Schematic of the circulation metrics studied in this paper. The black lines and symbols are for the present-day-like control simulation with disabled cloud-radiative interactions. The red lines and symbols show changes that are robust across models when cloud-radiative interactions are enabled. For example, the cloud-induced increase in the Hadley cell strength Ψ is depicted by a larger red cross, and the decrease in tropical-mean precipitation $\bar{P}$ and increase in equatorial peak precipitation P_{max} is depicted by fewer red rain drops that are concentrated closer to the equator. The other symbols are defined in section 2.2 and the caption of Table 1. HC = Hadley cell.

Table 2
Change in the Tropical Circulation in Response to 4K Surface Warming

	Model	Ψ	$\bar{\omega}^{\uparrow}$	$\bar{\omega}^{\downarrow}$	φ^{HC}	$\varphi^{\uparrow}$	$\varphi^{\downarrow}$	$\bar{P}$	P_{max}
A	CNRM-CM5	−12.9/−0.3	−1.7/−0.1	−3.3/−0.5	1.6/0.3	0.6/0.0	1.0/0.3	0.5/0.6	0.9/1.6
B	HadGEM2-A	−43.6/−16.1	−8.9/−1.2	−3.7/−3.4	1.6/1.5	0.5/−0.4	1.0/1.9	0.5/0.6	1.0/1.9
C	IPSL-CM5A-LR	−8.6/−26.4	−2.7/−2.4	−2.1/−3.2	1.9/1.0	0.5/0.3	1.4/0.7	0.6/0.6	1.1/1.4
D	MIROC5	−61.2/−27.4	−8.5/−3.1	−4.7/−2.7	1.5/1.9	0.8/1.1	0.7/0.8	0.5/0.7	−0.3/1.1
E	MPI-CM5-LR	5.4/−6.1	10.5/0.6	−2.9/−2.0	1.3/1.8	−1.7/1.0	3.0/0.8	0.5/0.6	9.0/2.5
F	MRI-CGCM3	−25.6/−19.3	−0.8/0.6	−2.4/−2.5	1.3/1.4	0.0/−0.4	1.3/1.9	0.6/0.6	4.9/3.6
Ga	ICON-DWD	6.0/−13.9	4.4/−1.4	−3.1/−2.1	1.8/1.6	−1.2/0.4	3.0/1.2	0.5/0.5	3.5/1.7
Gb	ICON-MPI	−13.2/−7.8	−1.2/−1.4	−3.7/−3.0	1.6/1.3	0.2/0.7	1.4/0.6	0.7/0.8	3.1/2.1

Note. The values are calculated from the 4K minus the control simulations. The first number is for the clouds-on setup and the second for the clouds-off setup. The cloud-radiative impact on the response to surface warming is given by the difference between the first and second numbers. The meaning of the symbols is as in Table 1.

3. Impact of Cloud-Radiative Interactions on the Present-Day-Like Circulation

We start with how the presence of cloud-radiative interactions impacts the tropical circulation. We consider the CTRL simulations an idealized representation of the present-day climate and study the difference between the onCTRL and offCTRL simulations. We also studied the impact of cloud-radiative interactions in the 4K simulations and found the same qualitative results (Table 1; cf. supporting information Table S1 for relative changes).

Cloud-radiative interactions lead to several circulation changes that are robust across models (Table 1). These include a stronger and narrower ascent, a wider descent, a decrease in tropical-mean precipitation, and an increase in peak precipitation. The IPSL-CM5A-LR shows a weaker Hadley cell in terms of Ψ, but a closer look reveals that also in this model the mass stream function strengthens in the lower free troposphere (Figure 9 of Harrop & Hartmann, 2016). Moreover, a stronger Hadley cell was found by Watt-Meyer and Frierson (2017) in the CTRL simulations of three additional models. We therefore consider the strengthening of the Hadley cell by cloud-radiative interactions a robust cloud impact. Note that in MIROC5, the Qobs SST profile was used for the clouds-off simulations, whereas the clouds-on simulations used a SST profile with steeper gradients around the equator (Fläschner, 2016). Thus, the ascent narrowing and Hadley cell strengthening found in MIROC5 partly result from SST changes, explaining the comparably strong circulation response in that model.

The impact of cloud-radiative interactions on other circulation metrics is not robust across models. Cloud-radiative interactions cause stronger descent in some models but weaker descent in others. They lead to an up to 3° lat narrower Hadley cell in some models but a slightly wider Hadley cell in others. The non-robust impact on the Hadley cell width results from opposing changes in the ascent and descent widths. In some models, the ascent narrowing is larger than the descent widening and smaller in others.

We propose four simple reasons that help to understand the robust impacts of cloud-radiative interactions in a qualitative manner. To this end, we make use of understood properties of the tropical-mean atmospheric energy budget and the tropical atmosphere: radiative cooling is mainly balanced by condensational heating, tropical free-tropospheric temperatures are nearly uniform in the horizontal, tropical ACRE is dominated by high-level clouds associated with ascent and positive ACRE, and the Hadley circulation conserves mass.

We start from tropical-mean precipitation. We assume that precipitation is generated exclusively by ascending motion in the equatorial box of our two-box idealization of the tropical atmosphere (Figure 1). Tropical-mean precipitation, $\bar{P}$, can thus approximately be written as a function of tropical-mean ascent strength, $\bar{\omega}^{\uparrow}$, and the fraction of the tropical area covered by ascent, $A^{\uparrow}$:

$$\bar{P} = (\alpha\bar{\omega}^{\uparrow} + \beta)A^{\uparrow}. \tag{1}$$

With the small-angle approximation, $A^{\uparrow} \simeq \varphi^{\uparrow}/30°\text{lat}$. The parameters α and β connect the circulation to precipitation and are in units of millimeter per hectopascal and millimeter per day, respectively. We estimate α and β by calculating the probability density function of local precipitation as a function of local ω and approximating the ascending part by a linear fit of the form $P(\omega) = \alpha\omega + \beta$. This is done for each model and simulation individually. The probability density functions as well as the α and β values are shown in Figure S1 and Table S2.

Tropical-mean ACRE is positive, as it is dominated by high-level clouds. Therefore, when allowed to interact with radiation, clouds heat the tropical atmosphere and compensate for some of the radiative cooling of the atmosphere. Following the atmospheric energy budget (Fläschner, 2016; Harrop & Hartmann, 2016; Popp & Silvers, 2017), this reduces the need for condensational heating and leads to a decrease of $\bar{P}$ in the clouds-on configuration compared to the clouds-off configuration (Table 1). Knowing that

$$\delta\bar{P} < 0, \tag{2}$$

where δ is defined as the clouds-on minus clouds-off configuration; we combine equations (1) and (2) to express the fractional precipitation change due to the presence of cloud-radiative interactions relative to the clouds-off configuration as

$$0 > \frac{\delta\bar{P}}{\bar{P}} = \frac{\delta A^{\uparrow}}{A^{\uparrow}} + \frac{\alpha A^{\uparrow}}{\bar{P}}\delta\bar{\omega}^{\uparrow}. \tag{3}$$

The precipitation change due to the combined change in α and β is much smaller than the precipitation change due to changes in $\bar{\omega}^{\uparrow}$ and $A^{\uparrow}$ (Figure S2) and hence neglected. For reasons discussed below, $\delta\bar{\omega}^{\uparrow} > 0$. Thus, for $\bar{P}$ to decrease, $A^{\uparrow}$ must decrease. This explains the narrowing of the ascent and hence the ITCZ due to cloud-radiative interactions. It also explains the widening of the descent and hence the decrease in tropical-mean precipitation. This is because changes in the descent and ascent widths are negatively correlated in the COOKIE ensemble (correlation coefficient of -0.81 for CTRL SST and -0.93 for 4K SST), consistent with Coupled Model Intercomparison Project Phase 5 coupled models (Byrne & Schneider, 2016a). In contrast, changes in descent width are not strongly correlated to changes in Hadley cell width, and changes in Hadley cell width are not robust across models, likely because of opposite impacts of tropical and extratropical ACRE (Watt-Meyer & Frierson, 2017).

We now provide an argument for why cloud-radiative interactions strengthen the ascent. For this, we use the weak temperature gradient approximation (e.g., Thompson et al., 2017)

$$\omega = -\frac{Q_r + Q_c}{S}, \tag{4}$$

where Q_r is radiative heating, Q_c is heating due to phase changes of atmospheric water, and S is the static stability.

Averaging vertically over the free troposphere and horizontally over the ascent region and neglecting spatial variations in S, we arrive at

$$\bar{\omega}^{\uparrow} = \frac{g}{dp_{ft}c_p}\frac{\hat{Q}_r^{\uparrow} + L\bar{P}^{\uparrow}}{S} = \gamma\frac{\hat{Q}_r^{\uparrow} + L\bar{P}^{\uparrow}}{S}, \tag{5}$$

where g is the gravitational acceleration, dp_{ft} is the pressure thickness of the free troposphere, c_p is the heat capacity of air at constant pressure, and L is the latent heat of condensation. $\hat{Q}_r^{\uparrow}$ and $\bar{P}^{\uparrow}$ are the net radiative heating (units of $W * m^{-2}$) and precipitation (units of $kg \cdot m^2 \cdot s^{-1}$) averaged over the ascent region. By restricting the vertical average to the free troposphere, we neglect reevaporation of rain in the boundary layer, which we consider unproblematic given the qualitative nature of our arguments. Because we consider the mean over the ascent region, ω is replaced by $-\bar{\omega}^{\uparrow}$ in the above equation. Using $\bar{P}^{\uparrow} = \alpha\bar{\omega}^{\uparrow} + \beta$, that is, the version of equation (1) valid in the ascent region, we write equation (5) as

$$\bar{\omega}^{\uparrow} = \gamma\frac{\hat{Q}_r^{\uparrow} + L(\alpha\bar{\omega}^{\uparrow} + \beta)}{S}. \tag{6}$$

Further manipulation yields

$$\bar{\omega}^{\uparrow} = \gamma\frac{\hat{Q}_r^{\uparrow} + L\beta}{S - \gamma L\alpha}. \tag{7}$$

Equation (7) illustrates that the condensational heating associated with ascending motion can be regarded as a reduction in static stability and an increase in radiative heating, which both amplify the ascent in response to a radiative forcing. We finally write the fractional change in the ascent strength as

$$\frac{\delta\bar{\omega}^{\uparrow}}{\bar{\omega}^{\uparrow}} = \frac{\delta\hat{Q}_r^{\uparrow}}{\hat{Q}_r^{\uparrow} + L\beta} - \frac{\delta S}{S - \gamma L\alpha}, \tag{8}$$

where we again have neglected changes in α and β. In the context of the clouds-on versus clouds-off simulations, $\delta \hat{Q}_r^{\uparrow} \simeq ACRE > 0$ in the ascent region. Provided that the static stability does not change, cloud-radiative interactions thus lead to stronger ascent and thus an increase in peak precipitation. This is consistent with our approximations, as can be seen by rewriting equation (1) for local precipitation.

Equation (8) leaves the possibility that a large increase in static stability could lead to overall weaker ascent, but this is seen in none of the models. Equation (8) further illustrates that our arguments target the qualitative robust response and not the quantitative model differences therein. This is because models differ in S and δS, which contributes to the lack of correlation between ACRE and the cloud-induced strengthening of ascent (Figure S3).

Finally, we present an argument for why cloud-radiative interactions strengthen the Hadley circulation. In the framework of the two-box model, the Hadley cell strength Ψ is proportional to $\bar{\omega}^{\downarrow} A^{\downarrow}$. One might also use the analogous relation for the ascent strength and width, but the relation based on the descent is found to better correlate with the stream function-based estimate of the Hadley cell strength (Figure S4). With this, the relative change in the Hadley cell strength due to cloud-radiative interactions is

$$\frac{\delta \Psi}{\Psi} = \frac{\delta A^{\downarrow}}{A^{\downarrow}} + \frac{\delta \bar{\omega}^{\downarrow}}{\bar{\omega}^{\downarrow}}. \tag{9}$$

Changes in the descent strength differ in sign across models and in some models depend on SST. In contrast, there is a strong positive correlation across models between the widening of the descent and the Hadley cell strengthening (correlation coefficients of 0.89 for CTRL SST and 0.95 for 4K SST; Table 1). By mass conservation, the broader descent implies a stronger Hadley circulation. It is worth noting that IPSL-CM5A-LR is the only model in which cloud-radiative interactions weaken the Hadley cell. IPSL-CM5A-LR also shows the smallest increase in descent width and a comparably small decrease in ascent width (Table 1 and Table S1). This is consistent with the Hadley cell strengthening being driven by the cloud-induced widening of descent and narrowing of ascent.

4. Impact of Cloud-Radiative Interactions on the Tropical Circulation Response to Surface Warming

In this section we investigate the tropical circulation response to surface warming. Surface warming leads to a wider Hadley cell and wider and weaker descent for all models and both cloud configurations (Table 2; cf. Table S3 for relative changes), in line with previous studies with realistic model setups and with coupled atmosphere-ocean models (e.g., Frierson et al., 2007; Johanson & Fu, 2009; Lu et al., 2008, 2007; Seo et al., 2014). The response of the Hadley cell strength, the ascent strength, and ascent width is not robust across models and depends on the cloud configuration. Thus, the aquaplanet response is less consistent with previous studies that used coupled models and realistic boundary conditions and found the ascent to narrow and strengthen under global warming (e.g., Byrne & Schneider, 2016b; Lau & Kim, 2015). To study how cloud-radiative interactions affect the circulation response to surface warming, we compare the difference between the 4K minus CTRL simulations in the clouds-on and clouds-off configurations. The cloud impact is given by the difference between the first and second number in Table 2.

An important element of the arguments presented in section 3 is that tropical high-level clouds heat the atmosphere via $ACRE > 0$. Tropical high-level clouds increase in altitude with surface warming to maintain their cloud-top temperature (Hartmann & Larson, 2002). Because ACRE depends on the temperature difference between the surface and the cloud tops, the ACRE of tropical high-level clouds tends to increase in response to surface warming (Voigt & Shaw, 2016; Shaw et al., 2016). While one might expect that this leads to robust effects of cloud-radiative interactions on the circulation response to surface warming, this is not the case. The only robust impact of cloud-radiative interactions is a reduction of the increase in tropical-mean precipitation under surface warming (Table 2). Yet there is no significant correlation between the tropical-mean ACRE increase and the reduced precipitation increase due to surface warming in the clouds-on configuration across models (Figure S5).

The lack of robust impacts of cloud-radiative interactions on the circulation response to surface warming is in contrast to the robust cloud-radiative impact on the present-day-like circulation. We attribute this to three reasons. First, changes in ACRE between the CTRL and 4K simulations are small compared to the ACRE value
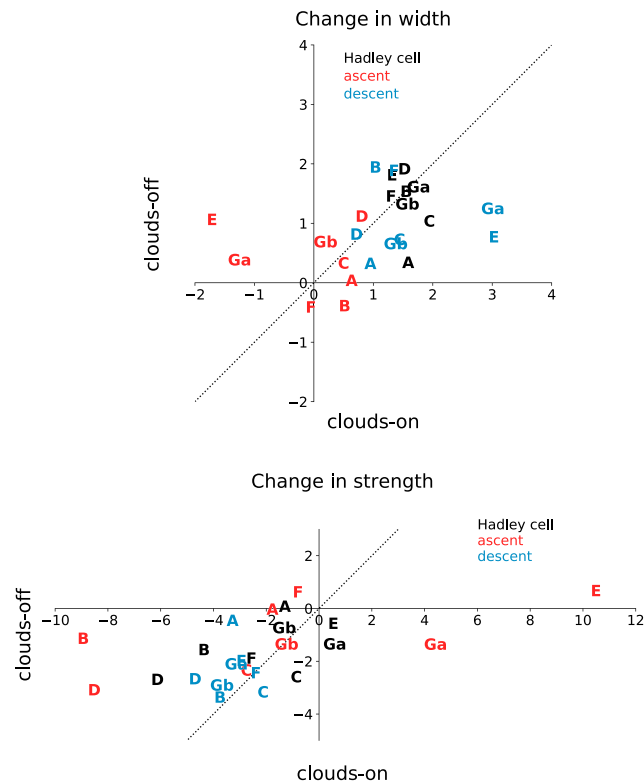
Figure 2. Surface warming-induced change in circulation widths in units of degree latitude (top) and in circulation strengths (bottom) in the clouds-on versus the clouds-off configurations. The ascent and descent strength are in units of hectopascal per day, the Hadley cell strength is in units of 10^{10} kg/s. The dashed lines mark the 1:1 lines. Models are distinguished by the letters listed in Tables 1 and 2.

in CTRL. Second, changes in tropical-mean ACRE are more complicated than a simple ACRE increase in the deep tropics (Figure S6). In some models (e.g., HadGEM2-A and IPSL-CM5A-LR), they involve changes in the subtropical ACRE. Other models (e.g., MIROC5 and MRI-CGCM3) show a decrease in deep-tropical ACRE, possibly due to a stability-induced reduction of the high-level cloud fraction (Bony et al., 2016). Third, changes in the circulation are not consistent with the picture developed in section 3. This can, for example, be seen by comparing ICON-MPI and CNRM-CM5A (Figure S6). ACRE increases near the equator in both models, but in ICON-MPI, cloud changes act to strengthen the ascent under surface warming and weaken it in CNRM-CM5A. We believe that this is because circulation-relevant factors such as vertical stability and atmospheric moisture content are not strongly impacted by the presence of cloud-radiative interactions in the present-day climate but change under surface warming (Shaw & Voigt, 2016). As a result, the cloud-radiative impact on the circulation response to climate change is smaller and more difficult to understand than the cloud-radiative impact on the present-day circulation.

Although cloud-radiative interactions have no robust impact on the circulation response to surface warming, they amplify the model spread in the response of the ascent and the response of the Hadley cell strength (Figure 2). Model spread in the clouds-on response of the ascent is 2–5 times larger than in the clouds-off response. In some models, cloud-radiative changes even change the sign of the ascent response. For example, in ICON-DWD, the ascent narrows and strengthens in the clouds-on but widens and weakens in the clouds-off configuration. Determining the reason for the increased model spread by cloud-radiative interactions is difficult, but the comparison between ICON-MPI and ICON-DWD points to parameterized cloud physics. In the clouds-off configuration, the ascent strength and width and the Hadley cell strength show a similar response in the two models but not in the clouds-on configuration (Figure 2). Regarding the descent and the Hadley cell width, clouds have no appreciable impact on the model spread. Overall, we find that cloud-radiative interactions primarily affect the surface-warming response of the ascent and the Hadley cell strength and have less of an impact on the descent and the Hadley cell width.

5. Discussion and Conclusions

We study the impact of cloud-radiative interactions on the tropical circulation and its response to surface warming using the COOKIE aquaplanet model ensemble expanded by the ICON model. The simulations study the ACRE, which predominantly arises from longwave radiation. For the present-day-like climate, cloud-radiative interactions lead to robust strengthening of the Hadley circulation and ascent, narrowing of the ascent and hence the ITCZ, and broadening of the descent.

We relate the robust cloud-radiative impacts to understood properties of the tropical atmosphere. Knowing that tropical-mean ACRE is positive, cloud-radiative heating counteracts the radiative cooling of the free troposphere and decreases tropical-mean precipitation. Cloud-radiative heating from tropical high-level clouds requires stronger adiabatic cooling and stronger ascent, which leads to an increase in peak precipitation. At the same time, because the ascent is strengthening, the reduction in tropical-mean precipitation requires a narrowing of the ascent region and the ITCZ. The narrower ascent region allows for a widening of the descent region and thus for a stronger downward mass flux in the subtropics and a stronger Hadley cell. The arguments that we put forward work in a qualitative manner but do not capture quantitative model differences in the qualitatively robust cloud impacts. This is not surprising given the approximations that are involved to derive them. While the arguments are not new individually, we present them here in a combined manner that highlights the importance of large-scale energetic constraints on the tropical circulation (cf. Popp & Silvers, 2017) and mirrors the energy budget considerations developed for the ITCZ position (e.g., Bischoff & Schneider, 2014; Donohoe & Voigt, 2017; Kang et al., 2009).

We also study how changes in cloud-radiative interactions affect the circulation response to surface warming (Ceppi & Hartmann, 2016; Ceppi & Shepherd, 2017; Voigt & Shaw, 2015, 2016). The analysis of the COOKIE ensemble in terms of climate change does not reveal robust cloud impacts, apart from the small decrease in the hydrological sensitivity (Fläschner et al., 2016). The lack of robust cloud-radiative impacts on the circulation response to surface warming is in contrast to Voigt and Shaw (2015) and Voigt and Shaw (2016), who applied the same aquaplanet setup as COOKIE but used the cloud-locking method. We suspect that the discrepancies in the COOKIE and locked-clouds approaches result from the fact that the cloud signal estimated from COOKIE includes changes in the reference state as well as water vapor, both of which can affect the circulation response (Kidston & Gerber, 2010; Voigt & Shaw, 2015). A detailed comparison of the COOKIE and cloud-locking approaches is planned for a future paper.

References

Bischoff, T., & Schneider, T. (2014). Energetic constraints on the position of the Intertropical Convergence Zone. *Journal of Climate*, *27*, 4937–4951. https://doi.org/10.1175/JCLI-D-13-00650.1.

Bony, S., Stevens, B., Coppin, D., Becker, T., Reed, K. A., Voigt, A., & Medeiros, B. (2016). Thermodynamic control of anvil-cloud amount. *Proceedings of the National Academy of Sciences of the United States of America*, *113*(32), 8927–8932. https://doi.org/10.1073/pnas.1601472113

Byrne, M. P., & Schneider, T. (2016a). Narrowing of the ITCZ in a warming climate: Physical mechanisms. *Geophysical Research Letters*, *43*, 11350–11357. https://doi.org/10.1002/2016GL070396

Byrne, M. P., & Schneider, T. (2016b). Energetic constraints on the width of the Intertropical Convergence Zone. *Journal of Climate*, *29*, 4709–4721. https://doi.org/10.1175/JCLI-D-15-0767.1

Ceppi, P., & Hartmann, D. L. (2016). Clouds and the atmospheric circulation response to warming. *Journal of Climate*, *29*, 783–799. https://doi.org/10.1175/JCLI-D-15-0394.1

Ceppi, P., & Shepherd, T. G. (2017). Contributions of climate feedbacks to changes in atmospheric circulation. *Journal of Climate*, *30*(22), 9097–9118. https://doi.org/10.1175/JCLI-D-17-0189.1

Donohoe, A., & Voigt, A. (2017). Climate extremes: Patterns and mechanisms, *Why future shifts in tropical precipitation will likely be small* (pp. 115–138). Hoboken: John Wiley. https://doi.org/10.1002/9781119068020.ch8

Fläschner, D. (2016). Intermodel spread in global and tropical precipitation changes, *Berichte zur Erdsystemforschung* (p. 183). Universität Hamburg: Hamburg. https://doi.org/10.17617/2.2321127

Fläschner, D., Mauritsen, T., & Stevens, B. (2016). Understanding the intermodel spread in global-mean hydrological sensitivity. *Journal of Climate*, *29*(2), 801–817. https://doi.org/10.1175/JCLI-D-15-0351.1

Frierson, D. M. W., Lu, J., & Chen, G. (2007). Width of the Hadley cell in simple and comprehensive general circulation models. *Geophysical Research Letters*, *18*, L18804. https://doi.org/10.1029/2007GL031115

Harrop, B. E., & Hartmann, D. L. (2016). The role of cloud radiative heating in determining the location of the ITCZ in aquaplanet simulations. *Journal of Climate*, *29*, 2741–2763. https://doi.org/10.1175/JCLI-D-15-0521.1

Hartmann, D. L., & Larson, K. (2002). An important constraint on tropical cloud—Climate feedback. *Geophysical Research Letters*, *29*, 1951. https://doi.org/10.1029/2002GL015835

Johanson, C. M., & Fu, Q. (2009). Hadley cell widening: Model simulations versus observations. *Journal of Climate*, *22*, 2713–2725.

Kang, S. M., Frierson, D. M. W., & Held, I. M. (2009). The tropical response to extratropical thermal forcing in an idealized GCM: The importance of radiative feedbacks and convective parameterization. *Journal of the Atmospheric Sciences*, *66*, 2812–2827. https://doi.org/10.1175/2009JAS2924.1

Kidston, J., & Gerber, E. P. (2010). Intermodel variability of the poleward shift of the austral jet stream in the CMIP3 integrations linked to biases in 20th century climatology. *Geophysical Research Letters*, *37*, L09708. https://doi.org/10.1029/2010GL042873

Lau, W. K. M., & Kim, K.-M. (2015). Robust Hadley circulation changes and increasing global dryness due to CO_2 warming from CMIP5 model projections. *Proceedings of the National Academy of Sciences of the United States of America*, *112*(12), 3630–3635. https://doi.org/10.1073/pnas.1418682112

Lu, J., Chen, G., & Frierson, D. M. W. (2008). Response of the zonal mean atmospheric circulation to El Niño versus global warming. *Journal of Climate*, *21*, 5942–5959.

Lu, J., Vecchi, G. A., & Reichler, T. (2007). Expansion of the Hadley cell under global warming. *Geophysical Research Letters*, *34*, L06805. https://doi.org/10.1029/2006GL028443

Medeiros, B., Stevens, B., & Bony, S. (2015). Using aquaplanets to understand the robust responses of comprehensive climate models to forcing. *Climate Dynamics*, *44*(7), 1957–1977. https://doi.org/10.1007/s00382-014-2138-0

Neale, R. B., & Hoskins, B. J. (2001). A standard test for AGCMs including their physical parametrizations: I: The proposal. *Atmospheric Science Letters*, *1*, 101–107. https://doi.org/10.1006/asle.2000.0022

Pierrehumbert, R. T. (1995). Thermostats, radiator fins, and the local runaway greenhouse. *Journal of the Atmospheric Sciences*, *52*(10), 1784–1806. https://doi.org/10.1175/1520-0469(1995)052%3C1784:TRFATL%3E2.0.CO;2

Popp, M., & Silvers, L. G. (2017). Double and single ITCZs with and without clouds. *Journal of Climate*, *30*(22), 9147–9166.

Randall, D. A., Harshvardhan, Dazlich, D. A., & Corsetti, T. G. (1989). Interactions among radiation, convection, and large-scale dynamics in a general circulation model. *Journal of the Atmospheric Sciences*, *46*, 1943–1970. https://doi.org/10.1175/1520-0469(1989)046<1943:IARCAL>2.0.CO;2

Scheff, J., & Frierson, D. M. W. (2012). Robust future precipitation declines in CMIP5 largely reflect the poleward expansion of model subtropical dry zones. *Geophysical Research Letters*, *39*, L18704. https://doi.org/10.1029/2012GL052910

Seo, K.-H., Frierson, D. M. W., & Son, J.-H. (2014). A mechanism for future changes in Hadley circulation strength in CMIP5 climate change simulations. *Geophysical Research Letters*, *40*, 5251–5258. https://doi.org/10.1002/2014GL060868

Shaw, T. A., Barnes, E., Baldwin, M., Caballero, R., Garfinkel, C., Hwang, Y.-T., et al. (2016). Storm track processes and the opposing influences of climate change. *Nature Geoscience*, *9*, 656–664. https://doi.org/10.1038/ngeo2783

Shaw, T. A., & Voigt, A. (2016). What can moist thermodynamics tell us about circulation shifts in response to uniform warming?. *Geophysical Research Letters*, *43*, 4566–4575. https://doi.org/10.1002/2016GL068712

Sherwood, S. C., Ramanathan, V., Barnett, T. P., Tyree, M. K., & Roeckner, E. (1994). Response of an atmospheric general circulation model to radiative forcing of tropical clouds. *Journal of Geophysical Research*, *99*, 20829–20845. https://doi.org/10.1029/94JD01632

Slingo, A., & Slingo, J. M. (1988). The response of a general-circulation model to cloud longwave radiative forcing. Part I: Introduction and initial experiments. *Quarterly Journal of the Royal Meteorological Society*, *114*, 1027–1062. https://doi.org/10.1002/qj.49711448209

Stevens, B., Bony, S., & Webb, M. (2012). Clouds On-Off Klimate Intercomparion Experiment (COOKIE). [Available at: http://www.euclipse.eu/wp4/wp4.html].

Su, H., Jiang, J. H., Zhai, C., Shen, T. J., Neelin, J. D., Stephens, G. L., & Yung, Y. L. (2014). Weakening and strengthening structures in the Hadley circulation change under global warming and implications for cloud response and climate sensitivity. *Journal of Geophysical Research: Atmospheres*, *119*, 5787–5805. https://doi.org/10.1002/2014JD021642

Taylor, K. E., Stouffer, R. J., & Meehl, G. A. (2012). An overview of CMIP5 and the experiment design. *Bulletin of the American Meteorological Society*, *93*, 485–498. https://doi.org/10.1175/BAMS-D-11-00094.1

Thompson, D. W. J., Bony, S., & Li, Y. (2017). Thermodynamic constraint on the depth of the global tropospheric circulation. *Proceedings of the National Academy of Sciences of the United States of America*, *114*(31), 8181–8186. https://doi.org/10.1073/pnas.1620493114

Voigt, A., Bony, S., Dufresne, J.-L., & Stevens, B. (2014). Radiative impact of clouds on the shift of the Intertropical Convergence Zone. *Geophysical Research Letters*, *41*, 4308–4315. https://doi.org/10.1002/2014GL060354

Voigt, A., & Shaw, T. A. (2015). Circulation response to warming shaped by radiative changes of clouds and water vapor. *Nature Geoscience*, *8*, 102–106. https://doi.org/10.1038/ngeo2345

Voigt, A., & Shaw, T. A. (2016). Impact of regional atmospheric cloud-radiative changes on shifts of the extratropical jet stream in response to global warming. *Journal of Climate*, *29*(23), 8399–8421. https://doi.org/10.1175/JCLI-D-16-0140.1

Watt-Meyer, O., & Frierson, D. M. W. (2017). Local and remote impacts of atmospheric cloud radiative effects onto the eddy-driven jet. *Geophysical Research Letters*, *44*, 10036–10044. https://doi.org/10.1002/2017GL074901

Zängl, G., Reinert, D., Ripodas, P., & Baldauf, M. (2015). The ICON (ICOsahedral Non-hydrostatic) modelling framework of DWD and MPI-M: Description of the non-hydrostatic dynamical core. *Quarterly Journal of the Royal Meteorological Society*, *141*, 563–579. https://doi.org/10.1002/qj.2378